Synthesis and Comparative Study on the Anti-Corrosion Potentials of Some Schiff Base Compounds Bearing Similar Backbone

[1,2,3]Elias E. Elemike, [1,2]Henry U. Nwankwo, [1,2*]Damian C. Onwudiwe

1. *Material Science Innovation and Modelling (MaSIM) Research Focus Area, Faculty of Agriculture, Science and Technology, North-West University, Mafikeng Campus, Private Bag X2046, Mmabatho 2735, South Africa.*
2. *Department of Chemistry, School of Mathematics and Physical Sciences, Faculty of Agriculture, Science and Technology, North-West University, Mafikeng Campus, Private Bag X2046, Mmabatho 2735, South Africa.*
3. *Department of Chemistry, College of Science, Federal University of Petroleum Resources, P.M.B 1221, Effurun, Delta State, Nigeria.*

* Corresponding author

Email: Damian.Onwudiwe@nwu.ac.za

Tel: +27 18 389 2545; Fax: +27 18 389-2420

Abstract

The synthesis of (*E*)-4-((p-tolylimino)methyl) phenol (TMPOL), (*E*)-4-((benzylimino)methyl) phenol (BMPOL) and (*E*)-4-((p-phenylimino)methyl) phenol (PMPOL) were carried out by the condensation reaction of 4-methylaniline, phenylmethanamine and aniline, respectively, with 4-hydroxybenzaldehyde. Molecular identities of the Schiff bases were probed using NMR (^{1}H and ^{13}C), Fourier transform infrared (FTIR) and mass spectroscopic techniques. The anticorrosion potency of these Schiff base compounds was investigated for mild steel (MS) in 1 M HCl solution using electrochemical methods. Potentiodynamic polarization (PDP) data revealed that all three compounds are mixed-type inhibitors, with TMPOL showing remarkable cathodic effect at high inhibitor concentrations. Electrochemical impedance spectroscopy (EIS) data revealed improved adsorption of inhibitor species on mild steel surface at elevated inhibitor concentrations. Scanning electron microscopy (SEM) reaffirmed the conditioning layer on the mild steel surface. Quantum chemical calculations provided molecular based explanations of the roles of heteroatoms and π electron centres on the corrosion inhibition activities of the studied Schiff bases. The better anticorrosion activities of BMPOL compared to its isomeric compound (TMPOL) can be ascribed to the presence of a

methylene linkage which enhanced the donor-acceptor interactions. The three inhibitors were inclined towards the Freundlich adsorption isotherm via a spontaneous chemical and physical adsorption of inhibitor molecules on MS surface.

Keywords: Schiff base; anticorrosion properties; electrochemistry; DFT

Introduction

The chemistry of corrosion process and the quest to protect metal from corrosion is a great concern among chemists and material scientists. There are continuous research and efforts to inhibit the corrosion process of metals, especially steel, due to their wide application in different industrial process and fluid transport. Organic compounds have in recent times emerged as promising candidates for metal protection, with special interest on the compounds that can be easily synthesized using low cost substrates and the compounds which posses high concentration of electron cloud on the aromatic ring and or rich electronegative atoms [1-2].

Schiff bases are recently emerging as compounds of interest in the application as corrosion inhibitors due the characteristic C=N bond which are formed through simple and straight forward procedure. Moreover, the C=N bond, in addition tothe aromatic rings present in some molecules, create rich electron platform that facilitates the adsorption of the compound on the metal surface thereby blocking the corrosion sites and preventing metal dissolution [3, 4]. There are many studies, including some of our reports, on the use of Schiff bases for metal corrosion prevention and most of the reports are recent which reflects the recent trend in the application of diverse Schiff base compounds as corrosion inhibitors [5-15]. The merit of using such compounds is the relative ease with which their structures can be modified by introducing special groups of atoms, thereby varying their properties and and producing compounds with enhanced properties [16].

The chemistry of corrosion inhibition using organic compounds, with high density of electrons on the electronegative atoms and on the pie-bonds present in the aromatic rings, is all about chelate formation on the metal surface. This is due to the electron donation from the electron-rich substrates or ligands resulting in dative bond through chemisorption process [17-22]. The ligand substrate has the electron rich centers such as the heteroatoms (N, S, O, P) which are nucleophilic, while the metal surface is electrophilic and ready to accept or share electrons. The inhibition capacity or adsorption efficiency is a function of the molecular structure of the compound, planarity of atoms or bulkiness of the group, types of heteroatoms present, type of electrolyte, the nature and surface morphology of

metal, the distribution of charge over the ligand inhibitor molecule and the type of aggressive media etc [23-26].

In order to explicitly explain the behaviour of the molecules and electron interaction within the individual groups, computational chemistry using the relatively common, easy and less expensive density functional theory (DFT) has been incorporated in this study [27]. The DFT, among other applications, helps in explaining the role of electrons on the corrosion inhibition offered by the Schiff base compounds. The quantum chemical parameters derived from the DFT such as energy of the highest occupied molecular orbitals E_{HOMO}, energy of the lowest unoccupied molecular orbital E_{LUMO}, energy difference ΔE, ionization energy (IE) etc are good descriptors that relate the nature of the molecules to their performance either as corrosion inhibitors or in other applications [28].
This work reports some Schiff base compounds with similar moiety and slight difference in their substituents groups, in order to evaluate their different potentials towards corrosion inhibition and the resultant effect of the substituents on their efficiency. It is intended that the work presented will help explain the effect of isomerism on the electrochemical activities of the studied Schiff bases.

Experimental

Materials

The starting materials, 4-methylaniline, 4-hydroxybenzaldehyde, benzylaniline, aniline were used as received from the supplier (Merck) without further purification.

Spectral, electrochemical measurements and theoretical modelling

Spectral characterisations of the compounds were carried out using Bruker alpha-P FTIR spectrophotometer operated at wavenumber range of 400-4000 cm^{-1}; the different proton and carbon environments were analysed using 600 MHz Bruker Avance III NMR spectrometers (at room temperature and DMSO as the solvent). The molecular weight of the compounds was obtained using micrOTOF-Q 1110390 Bruker compass mass spectrometer.
The study of corrosion inhibition of the Schiff bases on mild steel in aggressive acid medium was carried out using potentiodynamic polarization (PDP) and electrochemical impedance spectroscopy (EIS). Three-electrode system comprising mild steel, platinum rod and Ag/AgCl with 3 M KCl were used as working, counter and reference electrodes respectively on an Autolab PGSTAT 302N obtained from Metrohm. The inhibitor concentrations in the range (20-100 ppm) were prepared using acetone and distilled water as co-solvent. The PDP measurements of MS substrate in inhibited and uninhibited medium were scanned from cathodic to the anodic directions in the potential range of ±250 mV, with a scan rate of 0.5 mVs^{-1}.

PDP tests were performed after 1800 s of MS immersion in the aggressive solutions. Corrosion current density values were, thereafter, used to calculate the inhibition efficiency (*%IE*$_{PDP}$) using the following equation:

$$\%IE_{PDP} = 100\left(\frac{1-i_{corr}}{i^{o}_{corr}}\right) \quad (1)$$

where i^{o}_{corr} and i_{corr} are corrosion current densities without and with inhibitors respectively.

The EIS tests were achieved at the OCP by resolving the frequency response of the corrosion set-up in the range of 10 mHz to 100 kHz at 10 mV amplitude. The EIS data were fitted into appropriate equivalent circuit to obtain relevant electrochemical indices such as the charge transfer resistance (R_{ct}). The R_{ct} values were used to evaluate the *%IE*$_{EIS}$ using the formula:

$$\%IE_{EIS} = 100\left(\frac{R_{ct}-R^{o}_{ct}}{R_{ct}}\right) \quad (2)$$

where R_{ct} and R^{o}_{ct} are the charge transfer resistances with and without inhibitor respectively.

Gaussian 09W software package on B3LYP functional and basis set of a 6-31G+ were used for quantum chemistry calculations [29]. Extensive geometry optimization calculations were performed on the Schiff bases in both gas and aqueous phases. The water effect on the electronic indices of the studied Schiff bases was probed using the polarizable continuum model [30]. The quantum indices recorded are the energy of the lowest unoccupied molecular orbital (*E*$_{LUMO}$), the energy of the highest occupied molecular orbital (*E*$_{HOMO}$), energy band gap ($\Delta E = E_{LUMO} - E_{HOMO}$), chemical hardness ($\eta$), chemical softness ($\sigma$) and dipole moment. Most of these were derived from the *E*$_{HOMO}$ and *E*$_{LUMO}$ using the following equations (equations 3-5) [30]:

$$\Delta E = E_{LUMO} - E_{HOMO} \quad (3)$$

$$\eta = -\frac{1}{2}\left(E_{HOMO} - E_{LUMO}\right) \quad (4)$$

$$\sigma = \frac{1}{\eta} = -\left(\frac{2}{E_{HOMO} - E_{LUMO}}\right) \quad (5)$$

Synthesis of compounds: (*E*)-4-((p-tolylimino)methyl) phenol (TMPOL), (*E*)-4-((benzylimino)methyl) phenol (BMPOL), and (*E*)-4-((p-phenylimino)methyl) phenol (PMPOL)

The Schiff base compounds were prepared by refluxing the respective primary amines with 4-hydroxybenzaldehyde. About 10 mmol of the following amines: 4-

methylaniline, phenylmethanamine, and aniline were utilized in a 1:1 molar ratio with for 4-hydroxybenzaldeyde in ethanol and 2-3 drops of glacial acetic to obtain BMPOL, and PMPOL respectively acid after 2 h at a temperature of about 90 ^{o}C . After cooling, the products were filtered out and dried.

TMPOL: Yield, 59.25%. Selected FTIR (cm^{-1}): 3024 υ(H-C=), 2913, 2858 υ(H-C-), 1604 υ(C=N), 1573,1513s υ(C=C), 1385 (Ar-OH), 1189 (Ar-C-H), 837 (p-benzene ring).
^{1}H NMR: (DMSO, δ ppm): 2.49 (s, CH_3), 6.85, 6.93, 7.17, 7.75 (m, C_6H_4), 8.42 (s, N=CH), 9.76 (s, OH). ^{13}C NMR (DMSO, δ ppm): 20.60 (CH_3), 114.17, 124.30, 128.10, 130.64, 134.11, 146.10, 159.24 (C_6H_4), 163.43 (HC=N), 191.16 (C-OH). MS (ESI) m/z = $C_{14}H_{13}NO$. Calcd, 211.26; Found $[M+H]^+$ 212.10 (100%). Anal. cal for $C_{14}H_{13}NO$: C, 79.59; H, 6.20; N, 6.63; Found: C, 78.95; H, 6.59; N, 6.84%.

BMPOL: Yield, 59.41%. Selected FTIR (cm^{-1}): 3027 υ(H-C=), 1628,1601 υ(C=N), 1580, 1494 υ(C=C), 1307 (Ar-OH), 1169 (Ar-C-H), 987 (p-benzene ring). ^{1}H NMR: (DMSO, δ ppm): 4.95 (s, CH_2), 6.54, 7.17, 7.28, 7.39, 7.74 (m, C_6H_4), 8.45 (s, N=CH), 9.78 (s, OH). ^{13}C NMR (DMSO, δ ppm): 76.77 (CH_2), 115.75, 121.99, 124.28, 133.45, 136.36, 138.31, 145.28, (C_6H_4), 163.41 (HC=N), 191.14 (C-OH). MS (ESI) m/z = $C_{14}H_{13}NO$. Calcd, 211.26; Found $[M+H]^+$ 212.10 (100%). Anal. cal for $C_{14}H_{13}NO$: C, 79.59; H, 6.20; N, 6.63; Found: C, 79.05; H, 6.34; N, 6.99%.

PMPOL: Yield, 17.04%. Selected FTIR (cm^{-1}): 3030 (H-C=), 1600 υ(C=N), 1513 υ(C=C), 1282 (Ar-OH), 1188 (Ar-C-H), 838,(p-benzene ring). ^{1}H NMR: (DMSO, δ ppm): 6.88, 6.97, 7.18, 7.38, 7.77 (m, C_6H_4), 8.45 (s, N=CH), 9.77 (s, OH). ^{13}C NMR (DMSO, δ ppm): 115.91, 120.93, 127.95, 129.30, 130.72, 148.65, 152.04 (C_6H_4), 160.13 (HC=N), 191.06 (C-OH). MS (ESI) m/z = $C_{13}H_{11}NO$. Calcd. 197.23; Found $[M+H]^+$ 198.09 (100%). Anal. cal for $C_{13}H_{11}NO$: C, 79.17; H, 5.62; N, 7.10%; Found: C, 79.34; H, 5.05; N, 7.31%.

2.4. Mild steel preparation for corrosion studies and material surface analysis

The compositions of MS coupons used for electrochemical corrosion tests were as follows: P, S, Si, C and Fe with percentage weights of 0.019, 0.017, 0.46, 0.17 and 99.334 %, respectively. MS coupons of 1 cm x 1 cm dimension were used. The MS coupons were partially suspended in a molten Teflon holder and allowed to solidify leaving an exposed surface area of 1 cm^2. Before measurement was taken, the MS surface was scraped on Struers MD PianoTM 220. The surface was further abraded using increasing smoother SiC papers of grit size up to 600 to obtain a shiny surface, followed by sonicating in acetone and alcohol bath. The cleaned MS specimens were air-dried and used as the working electrode in the electrochemical

tests. For SEM analyses, the cleaned MS coupons were immersed in 1 M HCl solution with and without 100 ppm of the reported Schiff bases. After 4 h immersion period, the specimens were retrieved, cleaned with distilled water, dried and used for SEM analyses.

Results and Discussion

Synthesis

The three Schiff base compounds (BMPOL, TMPOL, PMPOL) were synthesized in ethanol solution, and they all gave yellowish colour which turned brownish yellow after drying. All the reactions were carried out in a 1:1 molar ratio as presented in Scheme 1(a-c). They are soluble in dichloromethane (DCM), ethanol, chloroform but insoluble in water . BMPOL and TMPOL are isomers, and gave almost the same moderate yield compared to the low yield of PMPOL.

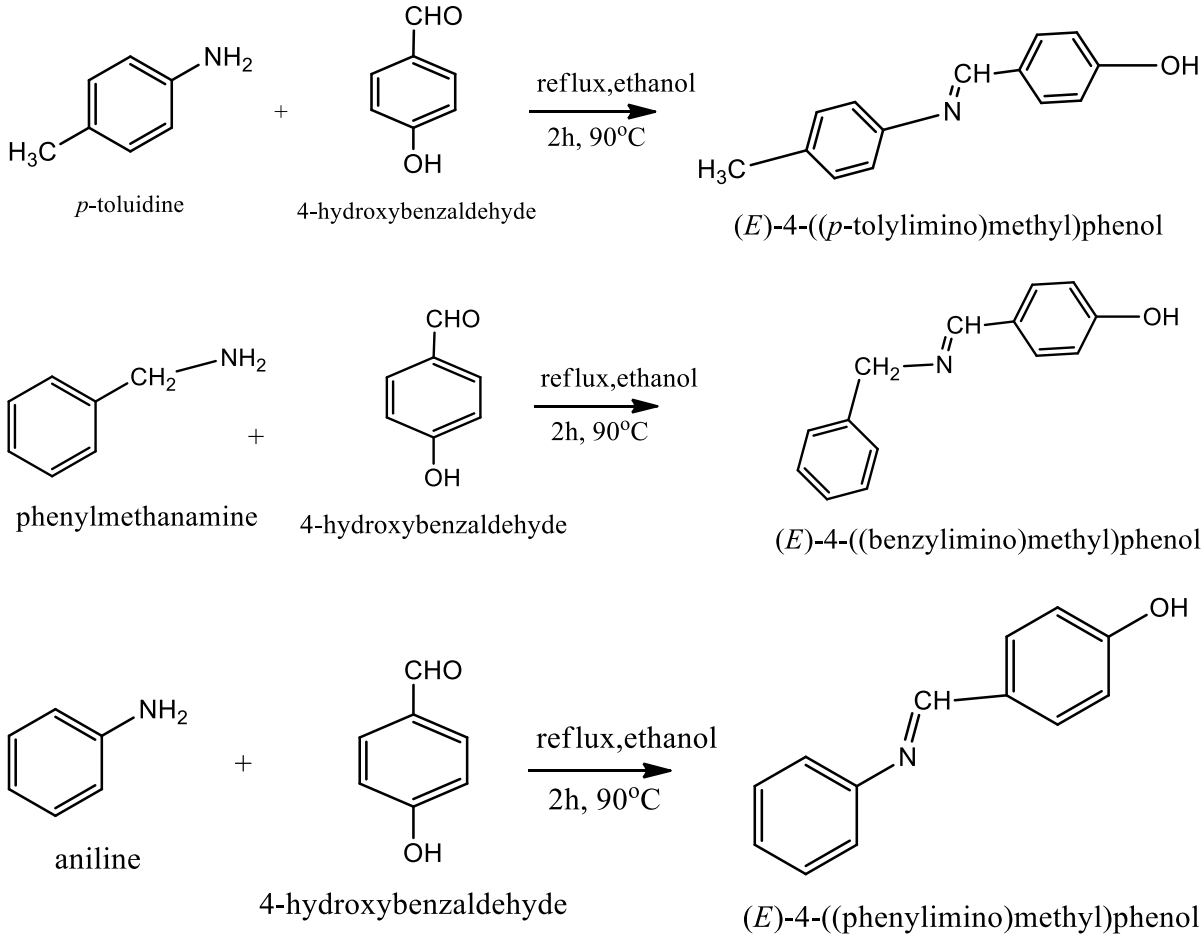

Scheme 1: Synthetic route for the synthesis of (a) BMPOL, (b) TMPOL, and (c) PMPOL.

FTIR studies

The absorption obtained around 3020-3030 cm^{-1} in all the compounds are major indications of unsaturation due to the C-H vibration of hydrogen attached to an SP^2 hybridized carbon. In the spectrum of TMPOL, the weak absorption at 3025 cm^{-1}, represents the vibrational frequency of the C-H bonds of the phenyl rings, the symmetrical and assymetrical vibration of the -C-H attached to a saturated carbon appeared at 2913 and 2858 cm^{-1} respectively. This could be ascribed to C-H of the methyl group attached in the para position of the aromatic ring. The C=N stretching vibrations was recorded at 1604 cm^{-1}. Other absorptions noticed around 1573, 1513 cm^{-1} could be due to aromatic ring stretch while the vibrations at 1385 cm^{-1} may be due to phenolic OH bend. The band around 1189 cm^{-1} could be attributed to aromatic C-H in plane bend while the intense bands noticed around 976, 819, 795 cm^{-1} are due to trans C-H out of plane bend and characteristic bands of the aromatic unsaturation [31].

In the spectrum of BMPOL, the aromatic =C-H vibrations were recorded at 3027 cm^{-1} while the C=N peaks appeared at 1628. The bands at 1528 and 1494 cm^{-1} are due to the aromatic stretching vibrations while the peak at 1307 cm^{-1} could be attributed to the O-H of the phenolic group. The other bands at 1080, 1025, 987 cm^{-1} could be attributed to secondary evidence of aromatic C-H in plane and out of plane bending vibrations coupled with p-substituted aromatic rings [31-33]. The spectrum of PMPOL gave weak absorption at 3030 cm^{-1} attributed to =C-H vibrations of the aromatic rings. The band due to the C=N group showed absorption around 1600 cm^{-1}. The phenolic O-H bending vibrations appeared at 1282 cm^{-1} while other bands, 1188, 838, 792 cm^{-1} are attributed to in plane and out of plane C-H bending vibrations.

NMR spectral studies

The ^{1}H and ^{13}C NMR spectra of the Schiff base compounds were recorded in DMSO. Different signals were obtained which described the structures of the synthesized Schiff base compounds. Signals at 2.49 ppm in TMPOL can be assigned to the methyl protons in the para position to the imine group. The aromatic protons appeared as multiplets between 6.85-7.75 ppm while the imino proton was observed at 8.42 ppm [32]. A deshielding effect was observed as a result the position of attachment of the OH proton, coupled with intramolecular hydrogen bonding that exist in the compound. This causes a chemical shift in the downfield region of 9.76 ppm. The ^{13}C NMR spectrum showed the signals due the methyl carbon at 20.60 ppm, and the peaks which appeared in the range114.17-159.24 ppm reflects the aromatic protons. The signal due to the imino carbon appeared at 163.43 ppm while the carbon bearing the OH reonated at 191.16 ppm. In the H NMR spectrum of

BMPOL, the absence of signals around 2 ppm signifies the absence of any proton due to aliphatic carbons. The spectrum showed chemical shift at 4.95 ppm which is an indication of methylene protons attached to an electron withdrawing group (imino), which exerts some deshielding effect. The aromatic protons occurred as multiplet in the region of 6.54-7.74 ppm, and the signal at 8.45 ppm could be attributed to the imino proton. The OH proton in BMPOL exhibited singlet signal at 9.78 ppm. In the ^{13}C NMR, the methylene carbon appeared at 76.77 ppm while the aromatic carbons signals showed between 115.75- 145.28 ppm. The imino carbon appeared at 163.41 ppm and the carbon bearing the hydoxyl group resonated in the downfield region around 191.14 ppm [32].

The NMR signals obtained for PMPOL are similar to the spectra observed for BMPOL and TMPOL, this affirm to the similarity in their backbone. There were no signals obtained between 2.00-5.00 ppm showing the absence of methyl and methylene protons. The aromatic protons were observed between 6.88-7.77 ppm as multiplets. The azomethine proton resonated at 8.45 ppm as singlet peak whereas the encountered intramolecular hydrogen bonding caused the OH proton to have a downfield shift at 9.77 ppm similar to the other two compounds. The ^{13}C NMR showed aromatic protons between 115.91-152.04 ppm, the imino carbon at 160.13 ppm and the OH bearing carbon displayed signal at 191.06 ppm.

Mass spectroscopic results

The mass spectra shown in Figures 1-3 reflect the molecular masses of the different synthesized Schiff base compounds. The TMPOL and BMPOL have the same mass spectra results with molecular ion peak of 212.10 because they are isomeric, whereas the PMPOL has molecular ion peak of 198.09. The molecular formula of the compounds were obtained from the mass spectroscopic measurements, and there were no other fragmentation patterns observed in all the spectra which probably suggests the stability of the compounds.

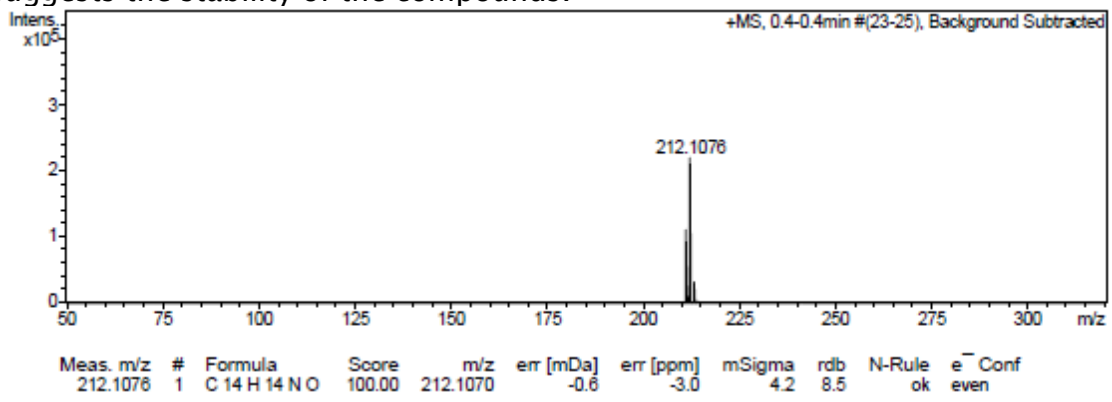

Figure 1: Mass spectrum of (*E*)-4-((p-tolylimino)methyl) phenol (TMPOL).

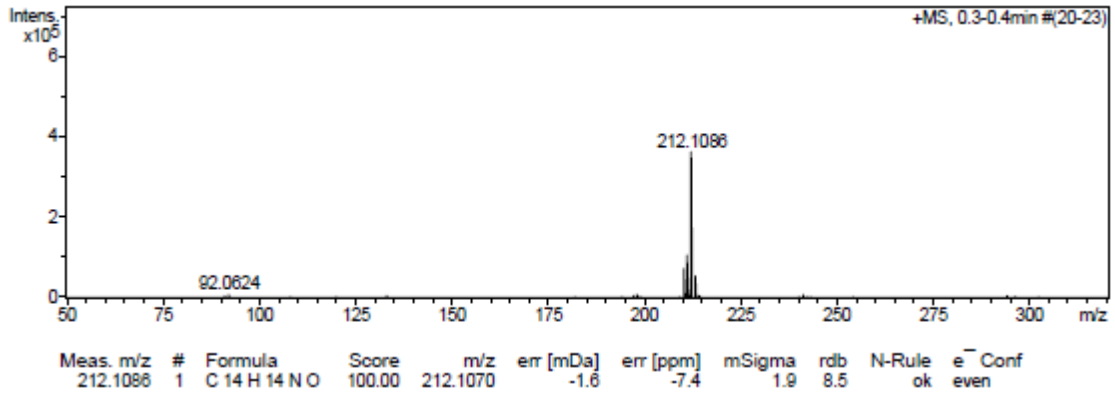

Meas. m/z	#	Formula	Score	m/z	err [mDa]	err [ppm]	mSigma	rdb	N-Rule	e¯ Conf
212.1086	1	C 14 H 14 N O	100.00	212.1070	-1.6	-7.4	1.9	8.5	ok	even

Figure 2: Mass spectrum of (*E*)-4-((benzylimino)methyl) phenol (BMPOL).

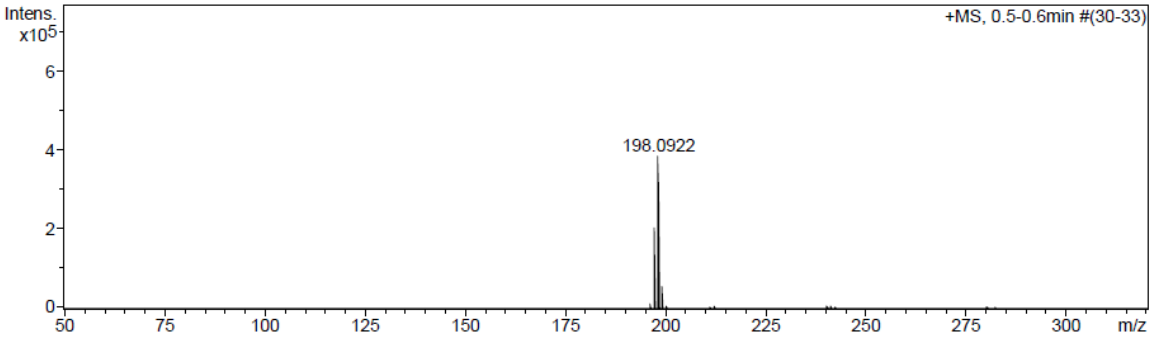

Meas. m/z	#	Formula	Score	m/z	err [mDa]	err [ppm]	mSigma	rdb	N-Rule	e¯ Conf
198.0922	1	C 13 H 12 N O	100.00	198.0913	-0.9	-4.3	1.3	8.5	ok	even

Figure 3: Mass spectrum of (*E*)-4-((p-phenylimino)methyl) phenol (PMPOL).

Tafel studies

Anodic and cathodic potentiodynamic polarisation was measured to establish the influence of inhibitors and change in concentration on the overall behaviour of MS in 1 M HCl solution [7, 30, 34, 35]. The results is presented in Figure 4 and the individual kinetic descriptors procured from the Tafel curves are recorded in Table 1.

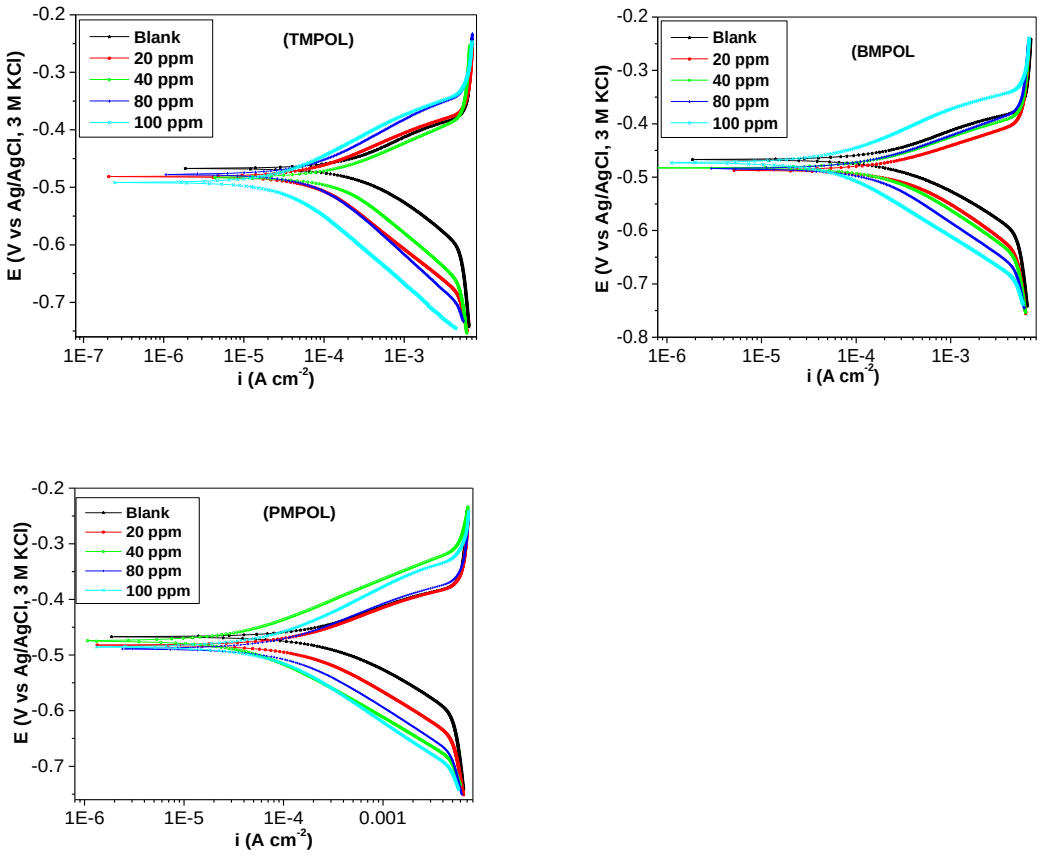

Figure 4: Tafel curves for MS in 1 M HCl without and with different concentrations of PMPOL, BMPOL and TMPOL.

The inhibitors display both cathodic and anodic effects on MS corrosion in 1 M HCl solution [8, 36]. A further investigation reveals that cathodic influence is more pronounced in TMPOL at maximum concentration (100 ppm), which resulted in the most significant reduction in current density recorded in the present study. In effect, PMPOL, BMPOL and TMPOL are all mixed type corrosion inhibitors but cathodic effect is more pronounced in TMPOL at elevated concentration [7, 8, 36]. The values of anodic (β_a) and (β_c) Tafel slopes recorded in Table 1 corroborate the observed effect on both cathodic and anodic arms of Figure 4. The minor shift in values of E_{corr} connotes that the present set of inhibitors retard MS dissolution by developing a defensive film that did not alter the reaction mechanism [7]. TMPOL recorded the least corrosion current density (i_{corr}) values at 20 ppm which suggests that TMPOL is a better corrosion inhibitor at the lowest studied concentration. However, there was a pronounced reduction in i_{corr} values for BMPOL at concentration range 80–100 ppm. Based on this observation, the obvious trend in inhibition efficiency obtained from averaged $\%IE_{PDP}$ values is such that BMPOL > TMPOL > PMPOL.

Table 1: Kinetic parameters from Tafel plots for MS in 1 M HCl in the absence and presence of PMPOL, BMPOL and TMPOL at various concentrations.

Conc (ppm)	β_a (mV/dec)	β_c (mV/dec)	$-E_{corr}$ (mV)	i_{corr} (μA cm^{-2})	$\%IE_{PDP}$
Blank	98.93	72.08	452.72	236	-
		PMPOL			
20	117.71	90.72	482.20	202	14
40	135.26	105.59	474.57	116	51
80	104.13	77.24	488.57	96	59
100	114.36	85.38	485.17	62	74
		BMPOL			
20	56.59	92.13	486.83	175	26
40	86.12	62.40	482.71	127	46
80	67.47	110.65	472.79	48	80
100	49.30	15.21	484.08	38	84
		TMPOL			
20	153.10	97.88	477.44	144	39
40	136.53	77.55	481.31	141	40
80	55.05	89.33	482.86	93	61
100	130.94	81.51	491.35	48	80

Impedance study

As shown in the Nyquist plots of Figure 5, the kinetics at interfaces can successfully be elucidated using EIS technique [7, 36]. The impedance spectrum registered at each concentration yielded imperfect semicircles in high frequency zone which implies charge transfer and development of defensive film on the MS surface [36, 37].

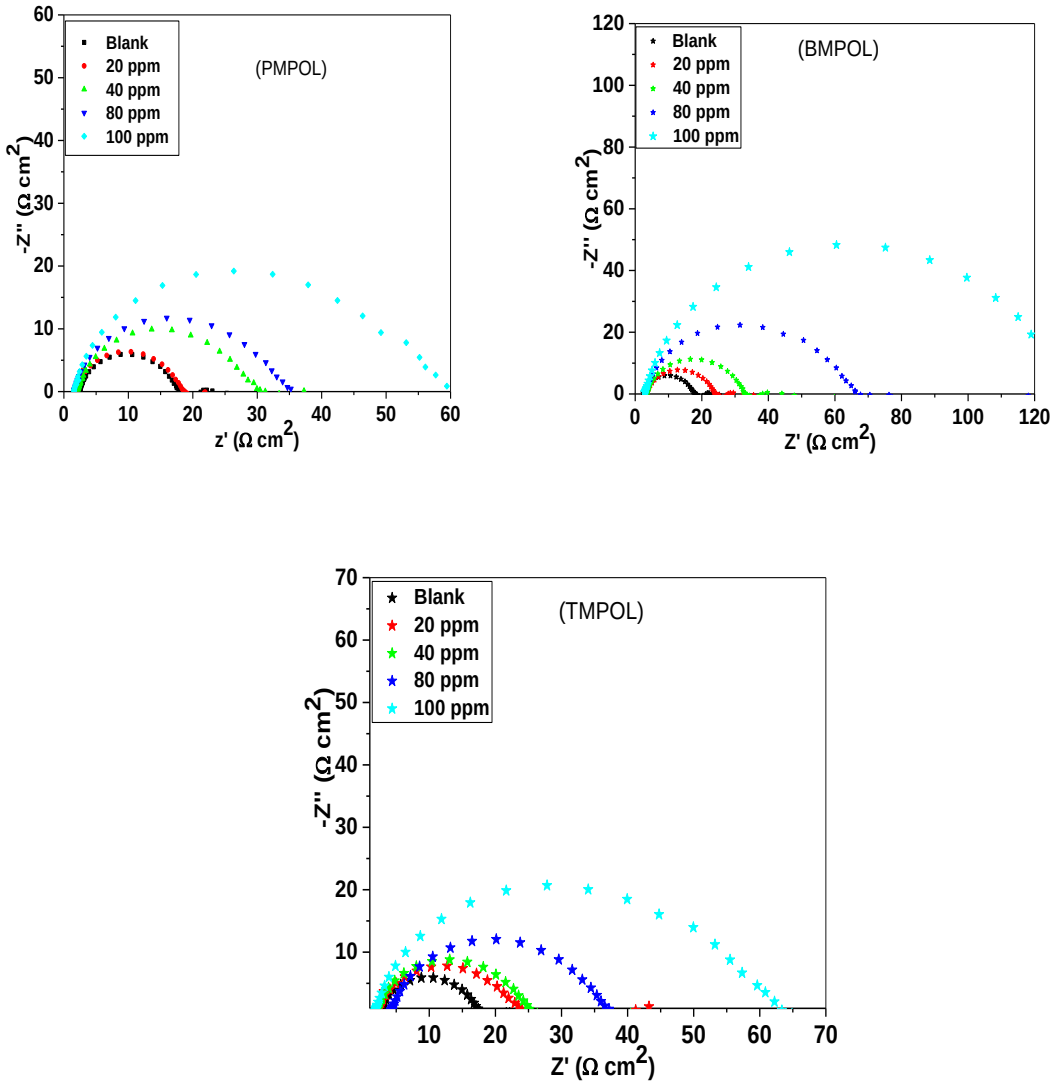

Figure 5: Impedance spectra for MS in 1 M HCl without and with different concentrations of PMPOL, BMPOL and TMPOL.

The imperfect nature of the semicircles arose from mass transfer processes, frequency dispersion and the obvious effect of MS rough surface [37, 38]. The overall impedance Z' for the inhibitor containing system has been shown to be higher than that obtained for the blank system. This suggests that electrochemical reactions may have taken place between the inhibitor and MS and/or between the inhibitor and the 1 M HCl solution (electrolyte) [39].

The impedance parameters which are recorded in Table 2 are used to describe the impedance characteristics of MS corrosion in blank and various concentrations of the studied Schiff bases [40-43]. The parameters were obtained after fitting the impedance data in a standard electrical equivalent circuit given in Figure 7 [30]. Herein, the constant phase element (*CPE*) was employed instead of the double layer

capacitance (C_{dl}) in order to achieve a more accurate fit. The capacitive nature of the imperfect semicircle in the present study was confirmed by the phase shift (n) values that tend to unity [30]. Slight increment in R_{ct} values was recorded for the inhibitors at low concentrations which suggest that the inhibitory activities of the reported compounds became significant only at elevated concentrations (80–100 ppm). This was further reaffirmed by the closeness of phase angle (α) and slope (S) values (Table 2) obtained for the blank and those of the inhibitor-containing systems especially at low concentrations. At improved concentrations however, there was an obvious improvement in α and S values that tend to -90 and -1 respectively. The deviation was due to the rough MS electrode surface and intricate electrochemical activities whereas the attempt to reach -90 and -1 mirrors an ideal capacitive electrode/electrolyte interface [30, 38]. The Bode phase angle plots in Figure 6 bear one time constant with widening of their maxima in the presence of inhibitor that suggests the formation of a protective layer on MS surface [30, 38]. The phenomenon supports the idea that at increased inhibitor concentrations, more inhibitor species adhere to the exposed surface of MS and make it more homogeneous. The magnitude of CPE constant (Y_0) and solution resistance (R_s) recorded minor changes with no clear trend. At concentrations range of 80–100 ppm, the values of R_{ct} follow the order of BMPOL > TMPOL > PMPOL, resulting to the inhibition efficiency order of: BMPOL > TMPOL > PMPOL, and the maximum $\%IE_{EIS}$ reaches up to 88%, 75% and 74% for BMPOL, TMPOL and PMPOL, respectively. These results reassure that the three Schiff bases possess good corrosion inhibition properties for MS in 1 M HCl solution. In addition, the $\%IE_{EIS}$ values display a similar trend to $\%IE_{PDP}$ values.

Table 2: Electrochemical parameters obtained from EIS plots for MS in 1 M HCl in the absence and presence of PMPOL, BMPOL and TMPOL at various concentrations.

Inhibitor	Conc (ppm)	R_s (Ω cm^{-2})	R_{ct} (Ω cm^{-2})	Y_0 ($\mu S s^n$cm^{-2})	n	$\%IE_{EIS}$	$-\alpha$	$-S$
Blank	–	2.50	17	677	0.8	–	40	0.30
				PMPOL				
	20	1.92	19	675	0.8	11	49	0.45
	40	2.15	33	677	0.8	48		
	80	1.57	38	582	0.8	55		
	100	1.54	65	434	0.8	74	59	0.53
				BMPOL				
	20	3.53	22	521	0.8	23	39	0.53
	40	3.58	32	429	0.8	47		

80	3.18	70	374	0.8	76		
100	2.85	137	289	0.8	88	61	0.78
			TMPOL				
20	2.08	26	796	0.8	35	45	0.44
40	1.87	27	621	0.8	37		
80	4.08	38	489	0.8	55		
100	1.67	69	347	0.8	75	58	0.48

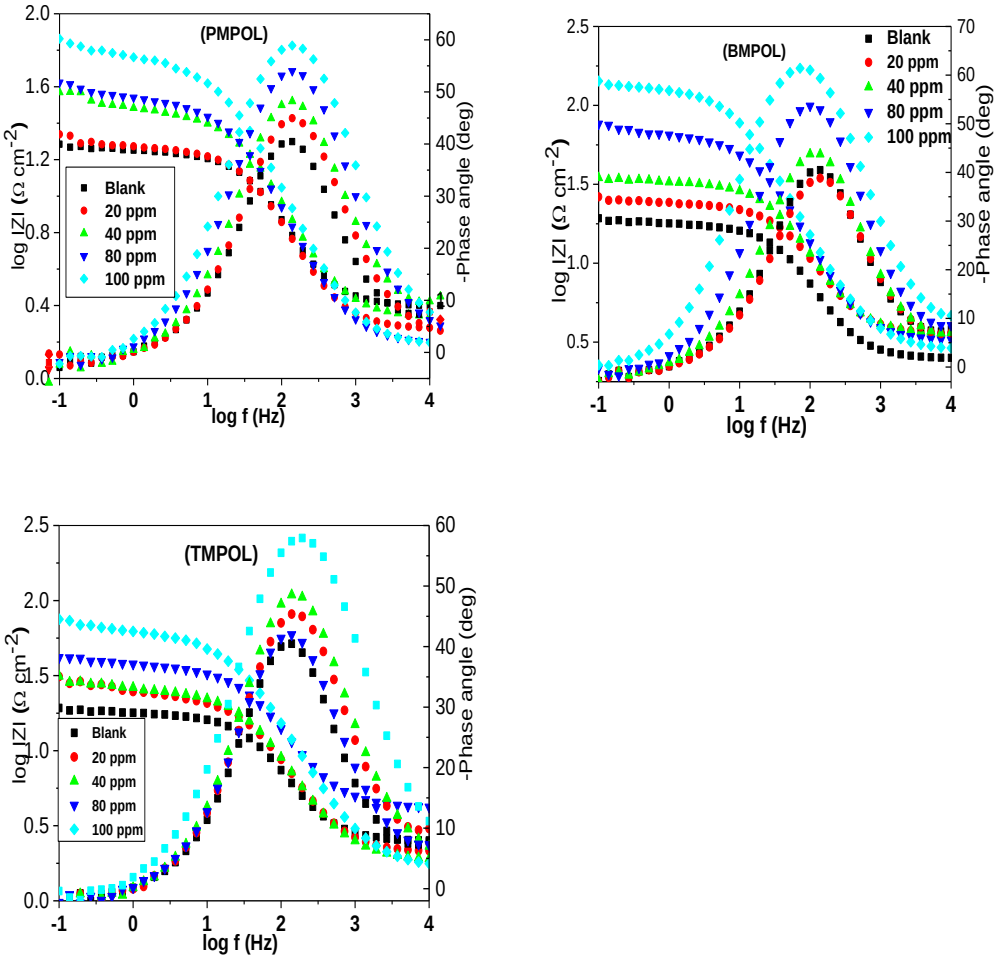

Figure 6: Bode impedance modulus and phase angle plots for MS in 1 M HCl in absence and presence of different concentration of PMPOL, BMPOL and TMPOL.

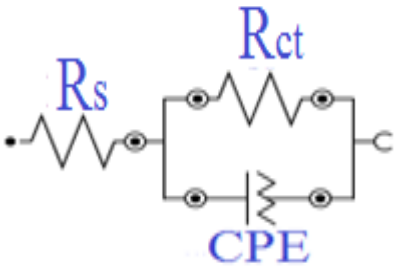

Figure 7: Electrochemical equivalent circuit.

Adsorption isotherm

Studying the adsorption isotherm of organic inhibitors on MS in acid solution was justified by the quasi-substitution action of the inhibitor specie that results in the formation of water-blocking matrix [38]. To explore the adsorptive behaviour of PMPOL, BMPOL and TMPOL on MS surface, different adsorption isotherms such as Freundlich, Frumkin and Langmuir have been examined to establish the potential link between inhibitor concentration (C) and the surface coverage ($\theta = C/\%IE_{EIS}$) shown in Table 2. We found that the adsorption of PMPOL, BMPOL and TMPOL molecules preferred the Freundlich isotherm of the form:

$$\theta = K_{ads} C_{inh} \tag{6}$$

where, θ is the degree of surface coverage; K_{ads} is the equilibrium constant of the adsorption/desorption activity and C_{inh} is the concentration of the inhibitor.

The fitting lines in Figure 8 show the Freundlich isotherm with values of slopes, intercepts and linear correlation coefficients (R^2) of the studied inhibitors. The choice of the Freundlich isotherm over the rest was based on the R^2 values that are almost unity and the intercept (I) at 0 [30].

Consequently, the values of K_{ads} were calculated from the intercept of the lines. The respective K_{ads} values are as follows: PMPOL: 28.2×10^5, BMPOL: 19.2×10^5 and TMPOL: 10.1×10^5. A higher K_{ads} value connotes a stronger interaction between adsorbate and adsorbent [37, 38]. As can be observed, the recorded K_{ads} values show that TMPOL is the least. This contradicts the weakest inhibition activity recorded for PMPOL on the acid corrosion of MS. A complex mode of physical and chemical interactions are usually impugned for such anomaly. The values of Gibb's free energy of adsorption, ΔG°_{ads} were obtained using the equation:

$$\Delta G^{\circ}_{ads} = -RT \ln(55.5 K_{ads}) \tag{7}$$

where, R is the universal gas constant, T is the absolute temperature and the value of 55.5 is the approximate concentration (in mol L^{-1}) of water in the solution. The recorded ΔG°_{ads} values are as follows: -47.5, -46.6 and -44.9 kJ.mol^{-1} that

represent PMPOL, BMPOL and TMPOL, respectively. The obtained ΔG°_{ads} values above the threshold of -40 kJ.mol^{-1} suggest a spontaneous process marked by both chemical and physical adsorption of inhibitor species on MS surface [44].

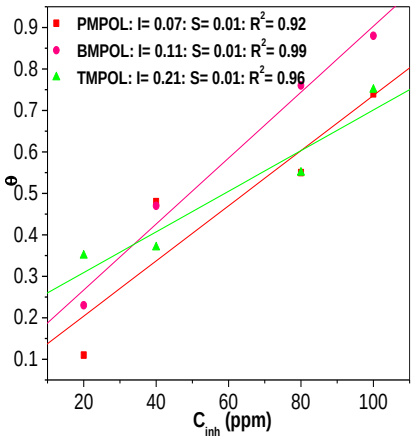

Figure 8: Adsorption isotherm plot of Freundlich for MS in the presence of PMPOL, BMPOL and TMPOL.

SEM studies

SEM images of MS specimens immersed in 1 M HCl for 3 h in the absence and presence of PMPOL or BMPOL or TMPOL are shown in Figure 9. As can be observed from Figure 9a, the MS surface recovered in blank solution bears a severely corroded image with densely distributed corrosion products. This is in sharp contrast to Figures 9b, 9c and 9d where the damage on the MS surface is slightly reduced, though with appearance of pits. This observation highlights the extent of protective potential of PMPOL, BMPOL and TMPOL as corrosion inhibitors for MS in acidic media. In effect, MS surfaces retrieved from the inhibitors are in a better condition even though the presence of the studied inhibitors initiated pitting cracks on MS specimens.

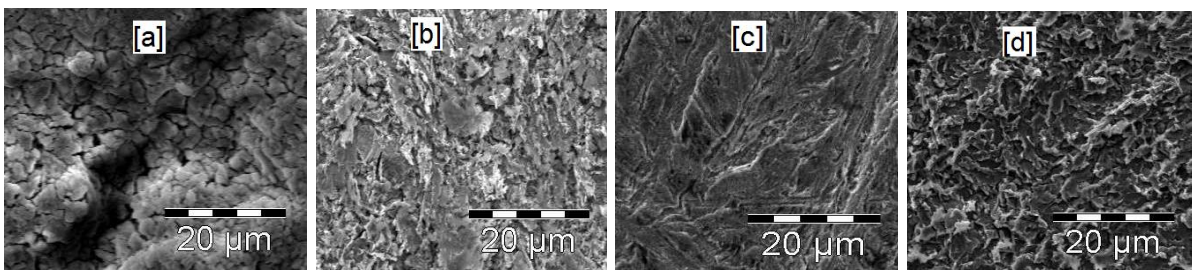

Figure 9: SEM images of MS samples after immersion in 1 M HCl for 3 h at 30 °C (a) without inhibitor, (b) with 100 ppm PMPOL, (c) with 100 ppm BMPOL and (d) with 100 ppm TMPOL.

Computational studies

The efficiency of organic molecules to act as corrosion inhibitors depends to a large extent on their structural and electronic properties [36, 37]. In exploiting these properties, the frontier molecular orbital (FMO) density distributions of non-protonated PMPOL, BMPOL and TMPOL were investigated in both gas and aqueous phases, as shown in Figure 10. The applicable quantum chemical descriptors most relevant to their corrosion inhibitory activities are listed in Table 3. In accordance with FMO postulate, molecular reactivity of molecules can be unravelled by analysis of the density distributions of HOMO and LUMO. E_{HOMO} elucidates the electron donating ability, whereas E_{LUMO} indicates the electron accepting ability of a molecule [7, 8, 30, 34-36]. Inspection of Figure 10 reveals that both the HOMO and LUMO are of π-type and spread over the entire structures of the Schiff bases except for BMPOL and TMPOL where there is little or no contribution from the phenyl π*-orbital and methyl alkyl chain to LUMO, respectively. Moreso, the contribution of O and N heteroatoms to LUMO and HOMO from the Schiff bases is evident. Therefore, the heteroatoms and Schiff base segment are the principal adsorption centers for donor-acceptor interactions with the unoccupied d-orbital of the iron atom to form coordinate bonds. Ideally, an efficient corrosion inhibitor is the molecule with the least energy gap (ΔE) [7, 30, 35], high dipole moment [30, 45], high chemical softness (·) [30, 35] and low chemical hardness (·) values [30, 46]. These quantum indices and their illustrations enhanced the reactivity of the studied inhibitors that hugely influenced donor-acceptor interactions with the mild steel, thereby shielding its surface from direct degradation in acid medium. Though there is no general trend of these quantum descriptors with the experimental corrosion inhibition efficiency of the studied inhibitors, most of them do however reaffirm that PMPOL is a better corrosion inhibitor for MS corrosion in 1 M HCl solution.

Optimised structure

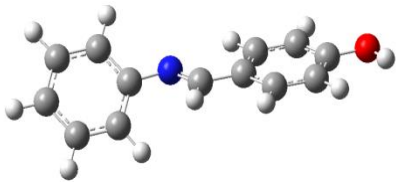
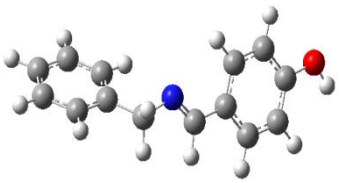
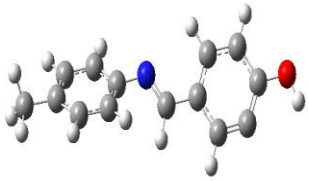

PMPOL BMPOL TMPOL

HOMO

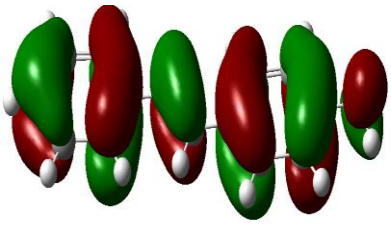
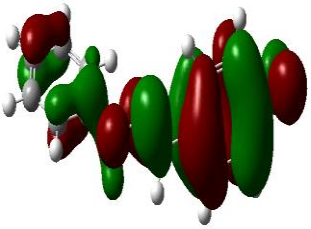
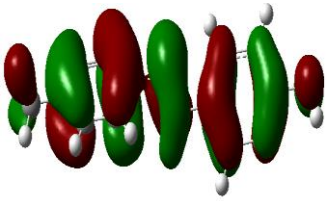

PMPOL BMPOL TMPOL

LUMO

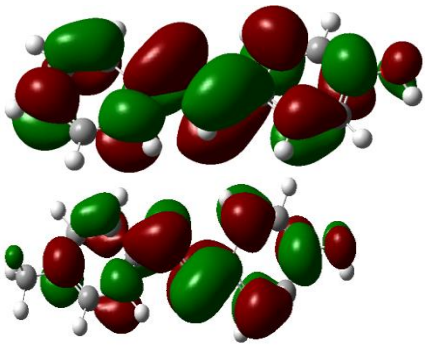
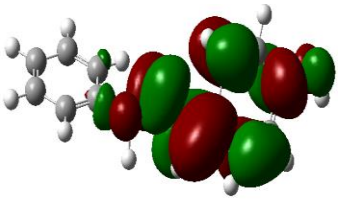

PMPOL BMPOL TMPOL

Figure 10: Optimised structures and FMO density distribution of the non-protonated inhibitors in gas phase.

Table 3: Selected quantum chemical parameters for the studied Schiff bases.

Inhibitor	E_{HOMO} (eV)	E_{LUMO} (eV)	ΔE (eV)	Dipole moment	·	·
			Gas Phase			
PMPOL	-5.99	-1.75	4.24	3.04	2.12	0.47
BMPOL	-6.30	-1.41	4.89	3.07	2.45	0.41
TMPOL	-5.93	-1.80	4.13	1.93	2.07	0.48
			Aqueous Phase			
PMPOL	-6.12	-1.88	4.24	4.47	2.12	0.47
BMPOL	-6.34	-1.49	4.85	4.05	2.43	0.41
TMPOL	-6.06	-1.93	4.13	2.96	2.07	0.48

Conclusion

The synthesis and characterization of (*E*)-4-((p-tolylimino)methyl) phenol (TMPOL), (*E*)-4-((benzylimino)methyl) phenol (BMPOL) and (*E*)-4-((p-phenylimino)methyl) phenol (PMPOL) have been reported in the present study. The Schiff bases are of a common structural backbone with different substituent groups attached to different centres. The cheaply synthesized compounds were investigated for corrosion inhibition activities against mild steel corrosion in 1 M HCl solution and the following conclusions can be drawn:

[1] TMPOL, BMPOL and PMPOL retard mild steel corrosion in 1 M HCl medium with their inhibition efficiency enhanced at increased inhibitor concentrations.

[2] Both polarization and impedance electrochemical techniques proved that the studied Schiff bases are mixed type corrosion inhibitors even though cathodic effect is more obvious in TIMP at elevated concentration.

[3] The adsorption of the inhibitors on mild steel was spontaneous, marked by both chemical and physical adsorption of inhibitor species and prefers the Freundlich adsorption isotherm.

[4] In the presence of the studied inhibitors, SEM images reveal improved surfaces that are devoid of an extensive layer of corroded porous film that marks the steel specimen immersed in 1 M HCl solution.

[5] Quantum chemical study indicates that heteroatoms and Schiff base segment are the principal adsorption centers for donor-acceptor interactions with the unoccupied d-orbital of mild steel. The better anticorrosion performance of BMPOL

and TMPOL can be attributed to among other factors to the presence of a methylene group and methyl alkyl chain, respectively.

References

1. "Plasma interface engineered coating systems for magnesium alloys" J. Zhang, Y. Chan, Q. Yu, *Prog. Org. Coat*. **61**, pp28-37, 2008.
2. "A Schiff base compound as effective corrosion inhibitor for magnesium in acidic media" D. Seifzadeh, H. Basharnavaz, A. Bezaatpour, *Mater. Chem. Phy*. **138**, pp794- 802, 2013
3. "Electrochemical investigation on the corrosion inhibition of mild steel by Quinazoline Schiff base compounds in hydrochloric acid solution" G. Khan, W. J. Basirun, S. N. Kazi, P. Ahmed, L. Magaji, S. M. Ahmed, G. M. Khan, M. A. Rehman,. *J. Col. Interf. Sci*. **502**, pp134-145, 2017.
4. "Corrosion inhibition of mild steel by some Schiff base compounds in hydrochloric acid" H. Ashassi-Sorkhabi, B. Shaabani, D. Seifzadeh, *Appl. Surf. Sci*. **239**, pp154-164, 2005.
5. "An experimental and theoretical investigation on adsorption properties of some diphenolic Schiff bases as corrosion inhibitors at acidic solution/mild steel interface" A. Yurt, B. Duran, H. Dal, *Arabian J. Chem*. **7**, pp732-740, 2014.
6. "Adsorption and Corrosion Inhibition Effect of Schiff Base Ligands on Low Carbon Steel Corrosion in Hydrochloric Acid Solution" N. Soltani, H. Salavati, N. Rasouli, M. Paziresh, A. Moghadasi, *Chem. Eng. Commun*. **203**, pp840-854, 2016.
7. "Synthesis, crystal structures, quantum chemical studies and corrosion inhibition potentials of 4-(((4-ethylphenyl)imino)methyl)phenol and (E)-4-((naphthalen-2-ylimino) methyl) phenol Schiff bases" E. E. Elemike, H. U. Nwankwo, D. C. Onwudiwe, E. C. Hosten, *J. Mol. Struct*. **1147**, pp252-265, 2017.
8. "Synthesis, crystal structure, electrochemical and anti-corrosion studies of Schiff base derived from o-toluidine and ochlorobenzaldehyde" E. E. Elemike, D. C. Onwudiwe, H. U. Nwankwo, E. C. Hosten, *J. Mol Struct*. **1136**, pp253-262, 2017.
9. "Synthesis, structures, spectral properties and DFT quantum chemical calculations of (E)-4-(((4-propylphenyl)imino)methyl)phenol and (E)-4-((2-tolylimino)methyl)phenol; their corrosion inhibition studies of mild steel in aqueous HCl" E. E. Elemike, H. U. Nwankwo, D. C. Onwudiwe, E. C. Hosten, *J. Mol. Struct.* **1141**, pp12-22, 2017.

10. "Synthesis, electrochemical and quantum chemical studies of some prepared surfactants based on azodye and Schiff base as corrosion inhibitors for steel in acid medium" M. A. Bedair, M. M. B. El-Sabbah, A. S. Fouda, H. M. Elaryian, *Corr Sci.* **128**, pp54-72, 2017.
11. "An example of green copper corrosion inhibitors derived from flavor and medicine: Vanillin and isoniazid" S. Mo, L. J. Li, H. Q. Luo, N. B. Li, *J. Mol. Liqs*. **242**, pp822-830, 2017.
12. "Corrosion inhibition of offshore oil and gas production facilities using organic compound inhibitors-A review" A. A. Olajire, *J. Mol Liqs*. **248**, pp775-808, 2017.
13. "Novel synthesized Schiff Base-based cationic gemini surfactants: Electrochemical investigation, theoretical modeling and applicability as biodegradable inhibitors for mild steel against acidic corrosion" H. M. Abd El-Lateef, K. A. Soliman, A. H. Tantawy, *J. Mol. Liqs*. **232**, pp478-498, 2017.
14. "Corrosion inhibition of carbon steel pipelines by some novel Schiff base compounds during acidizing treatment of oil wells studied by electrochemical and quantum chemical methods" H. M. Abd El-Lateef, A. M. Abu-Dief, M. A.A. Mohamed, *J. Mol. Str.* **1130**, pp522-542, 2017.
15. "Electrochemical and DFT studies of a new synthesized Schiff base as corrosion inhibitor in 1 M HCl" S. Benabid, T. Douadi, S. Issaadi, C. Penverne, S. Chafaa, *Measurement* **99**, pp53-63, 2017.
16. "Physicochemical studies on the inhibitive properties of a 1,2,4-triazole Schiff's base, HMATD, on the corrosion of mild steel in hydrochloric acid" P. R. Ammal, M. Prajila, A. Joseph, *Egypt. J. Petrol*. (2017), http://dx.doi.org/10.1016/j.ejpe.2017.05.002
17. "Schiff's base derived from 2-acetyl thiophene as corrosion inhibitor of steel in acidic medium" A. Aouniti, H. Elmsellem, S. Tighadouinia, M. Elazzouzi, S. Radi, B. A. Chetouani, B. Hammouti, A. Zarrouk *J. Taibah Univ. Sci.* **10**, pp774-785, 2016.
18. "Electrochemical and quantum chemical studies of some Schiff bases on the corrosion of steel in H_2SO_4 solution" R. Hasanov, M. Sadıkoglu, S. Bilgic, *Appl. Surf. Sci*. **253**, pp3913-3921, 2007.
19. "Aminic nitrogen-bearing polydentate Schiff base compounds as corrosion inhibitors for iron in acidic media: A quantum chemical calculation" H. Ju, Z-P. Kai, Y. Li, *Corr. Sci.* **50**, pp865-871, 2008.
20. "2-Hydrazino-6-methyl-benzothiazole as an effective inhibitor for the corrosion of mild steel in acidic solutions" M. Ajmal, A. S. Mideen, M. A. Quaraishi, *Corros. Sci*. **36**, pp79-84, 1994.
21. "Quantum chemistry study on the relationship between molecular structure and corrosion inhibition efficiency of amides" J. Fang, J. Li, *J. Mol. Str. (Theochem),* **593**, pp179-185, 2002.

22. "4-Amino-3-butyl-5-mercapto-1,2,4-triazole: a new corrosion inhibitor for mild steel in sulphuric acid" M. A. Quraishi, H. K. Sharma, *Mater. Chem. Phys*. **78**, pp18-21, 2002.
23. "The effect of *N*-(1-toluidine) salicylaldimine on the corrosion of austenitic chromium-nickel steel" S. Bılgıç, N. Calıskan, *Appl. Surf. Sci.* **152**, pp107-114, 1999.
24. "Asymmetrical Schiff bases as inhibitors of mild steel corrosion in sulphuric acid media. M. Hosseini, S. F. L. Mertens, M. Ghorbani, M. R. Arshadi" *Mater. Chem. Phys*. **78**, pp800-808, 2003.
25. "2-Butyne-1, 4-diol as a novel corrosion inhibitor for API X65 steel pipeline in carbonate/bicarbonate solution" E. S. Meresht, T. S. Farahani, J. Neshati, *Corros. Sci.* **54**, pp36-44, 2012.
26. "Adsorption and corrosion inhibition behaviour of N-(phenylcarbamothioyl) benzamide on mild steel in acidic medium" M. Gopiraman, N. Selvakumaran, D. Kesavan, R. Karvembu, *Prog. Org. Coat.* **73**, pp104-111, 2012.
27. "On the role of the electronic states of corrosion inhibitors: Quantum chemical-electrochemical correlation study on urea derivatives" M. E. Elshakre, H. H. Alalawy, M. I. Awad, B. E. El-Anadouli, *Corr. Sci*. **124**, pp121-130, 2017.
28. "Inhibition of mild steel corrosion in hydrochloric using three different 1,2,4-triazole Schiff's bases: A comparative study of electrochemical, theoretical and spectroscopic results" M. Prajila, A. Joseph, *J. Mol. Liqs*. **241**, pp1-8, 2017.
29. M. J. Frisch, *et al*. Gaussian 09, Revision C.01; Gaussian, Inc.: Wallingford, CT, USA, 2009.
30. "Experimental, quantum chemical and molecular dynamic simulations studies on the corrosion inhibition of mild steel by some carbazole derivatives" H. U. Nwankwo, L. O. Olasunkanmi, E. E. Ebenso, *Sci. Rep*. **7**, pp1-18, 2017.
31. "Interpretation of Infrared Spectra, A Practical Approach" R. A. Meyers (Ed.), *Encycl. Analyt. Chem.* John Wiley & Sons Ltd, Chichester, pp10815-10837, 2000.
32. "Co(II), Ni(II), Cu(II), and Zn(II) complexes derived from 4-[{3-(4-bromophenyl)-1-phenyl-1H-pyrazol-4-ylmethylene}-amino]-3-mercapto-6-methyl-5-oxo-1,2,4-triazine", K. Singh, R. Thakur, V. Kumar, *Beni-suef univ. J Basic Appl. Sci.* **5**, pp21-30, 2016.
33. "Synthesis and spectroscopic characterization of new tetradentate Schiff base and its coordination compounds of NOON donor atoms and their antibacterial and antifungal activity" M. S. Abdallah, M.A. Zayed, G. G. Mohamed, *Arabian J. Chem*. **3**, pp103-113, 2010.

34. "Synthesis, characterization, antimicrobial studies and corrosion inhibition potential of 1, 8-dimethyl-1, 3, 6, 8, 10, 13-hexaazacyclotetradecane: experimental and quantum chemical studies" H.U. Nwankwo, C.N. Ateba, L.O. Olasunkanmi, S. Abolanle, A.S. Adekunle, D.A. Isabirye, D.C. Onwudiwe, E.E. Ebenso, *Mater.* **9**, pp1-19, 2016.
35. "Experimental and Theoretical Study on the Inhibition Performances of Quinoxaline and Its Derivatives for the Corrosion of Mild Steel in Hydrochloric Acid" J. Fu, H. Zang, Y. Wang, S. Li, T. Chen, X. Liu, *Ind. Eng. Chem. Res*. **51**, pp6377−6386, 2012.
36. "Experimental and theoretical studies of (Z)-N-(2-chlorobenzylidene) naphthalen-1-amine and (Z)-N-(3-nitrobenzylidene)naphthalen-1-amine, and their corrosion inhibition properties" E. E. Elemike, H. U. Nwankwo, D. C. Onwudiwe, *J. Mol. Struct*., **1155**, pp123-132, 2018.
37. "Inhibition of mild steel corrosion in hydrochloric acid using two novel pyridine Schiff base derivatives: a comparative study of experimental and theoretical results" Y. Meng, W. Ning, B. Xu, W. Yang, K. Zhang, Y. Chen, L. Li, X. Liu, J. Zhenga, Y. Zhang, *RSC Adv*. **7**, 7, pp43014-43029, 2017.
38. "Amino acids modified konjac glucomannan as green corrosion inhibitors for mild steel in HCl solution" K. Zhang, W. Yang, X. Yina, Y. Chen, Y. Liu, J. Le, B. Xu, *Carbohydr. Polym*. **181**, pp191-199, 2018.
39. "Corrosion protection of magnesium by electroactive polypyrrole/paint Coatings" V. T. Truong, P. K. Lai, B. T. Moore, R. F. Muscat, M. S. Russo, *Synth. Met.,* **110**, pp7-15, 2000.
40. "In situ synthesis, electrochemical and quantum chemical analysis of an amino acid-derived ionic liquid inhibitor for corrosion protection of mild steel in 1M HCl solution" E. Kowsari, S. Y. Arman, M. H. Shahini, H. Zandi, A. Ehsani, R. Naderi, A. PourghasemiHanza, M. Mehdipour, *Corros. Sci*. **112**, pp73-85, 2016.
41. "Polysaccharide from Plantago as a green corrosion inhibitor for carbonsteel in 1 M HCl solution" M. Mobin, M. Rizvi, *Carbohydr. Polym.* **160**, pp172-183, 2017.
42. "Electrochemical and quantum chemical investigation of some Azine and Thiazine dyes as potential corrosion inhibitors for mild steel in hydrochloric acid solution" E. E. Ebenso, M. M. Kabanda, L. C. Murulana, A. K. Singh, S. K. Shukla, *Ind. Eng. Chem. Res*. **51**, pp12940-12958, 2012.
43. "Acenaphtho[1,2-b]quinoxaline and acenaphtho[1,2-b]pyrazine as corrosion inhibitors for mild steel in acid medium". J. Saranya, P. Sounthari, K. Parameswari, S. Chitra, *Measurement,* **77**, pp175-186, 2016.
44. "Adsorption and Corrosion Inhibition of Mild Steel by ((Z)-4-((2,4-dihydroxybenzylidene)amino)-5-methy-2,4 dihydro-3H-1,2,4-triazole-3-thione) in 1M HCl: Experimental and Computational Study" I. Merimi, Y. El

Ouadi, K. R. Ansari, H. Oudda, B. Hammouti, M. A. Quraishi, F. F. Al-blewi, N. Rezki, M. R. Aouad, M. Messali, *Anal. Bioanal. Electrochem.* **9**, pp640-659, 2017.

45. "Experimental and quantum chemical calculation studies on 2-[(4-Fluorophenylimino) methyl]-3,5-dimethoxyphenol" H. Tanak, A. Ağar, M. Yavuz, *J. Mol. Model.* **16**, pp577-587, 2010.
46. "Quinoxaline derivatives as corrosion inhibitors for mild steel in hydrochloric acid medium: Electrochemical and quantum chemical studies" L. O. Olasunkanmi, M. M. Kabanda, E. E. Ebenso, *Physica E* **76**, pp109-126, 2016.